Proactive Human-Manipulator collision avoidance through motion prediction and digital twin validation

Rajasundaram Mathiazhagan, Vadivelan Murugesan, Sanjana Joshi, Aliasghar Arab
Department of Mechanical and Aerospace Engineering, New York University

Abstract*— Safe human-robot collaboration in dynamic industrial environments poses significant challenges. In this work, a proactive collision avoidance framework is presented, integrating 3D human pose estimation, motion prediction, and digital twin simulation to prevent potential contact between human operators and robotic manipulators. Real-time skeletal joint data are extracted using a 3D depth camera and processed through MediaPipe for 3D joint localization. The extracted data are then passed through a neural motion forecasting model trained on joint trajectories. Predicted human motion is validated in a ROS 2-based digital twin environment where a UR16e robotic arm is spawned in both Gazebo and RViz. An A-RRT* planner, combined with Artificial Potential Fields (APF), is utilized to generate collision-free trajectories in response to forecasted human movements. Skeletal joints and robotic motion are visualized in RViz, facilitating intuitive real-time monitoring. Occlusion handling is achieved using autoencoders, and path replanning is performed within safety-critical time constraints. The proposed approach demonstrates effective integration of machine learning and simulation-driven methods for ensuring safe and intelligent human-robot interaction.

I. INTRODUCTION

As industrial robots become increasingly integrated into human-centric environments, enabling safe and intelligent interaction between humans and machines has emerged as a critical research challenge. In collaborative workspaces, robots must operate not only efficiently but also predictively—anticipating human motion and avoiding potential collisions proactively.

Traditional motion planning approaches are often reactive, responding to obstacles only after they are detected in close proximity. While effective in structured settings, these methods fall short in dynamic, human-shared environments where split-second decisions are required. To ensure continuous and safe task execution, predictive trajectory planning frameworks are essential.

This work presents a human-aware motion planning system for the UR16e robotic manipulator that integrates three key modules: human motion forecasting, artificial potential field (APF) evaluation, and real-time replanning using the Adaptive Rapidly-Exploring Random Tree Star (A-RRT*) algorithm. Human motion is predicted using a long short-term memory (LSTM)-based model, which provides a short-term forecast of future joint positions. These predicted poses are used to compute a repulsive APF score that quantifies potential collision risk. When this score exceeds a safety threshold, the A-RRT* planner is invoked to generate a new, collision-free trajectory in real time.

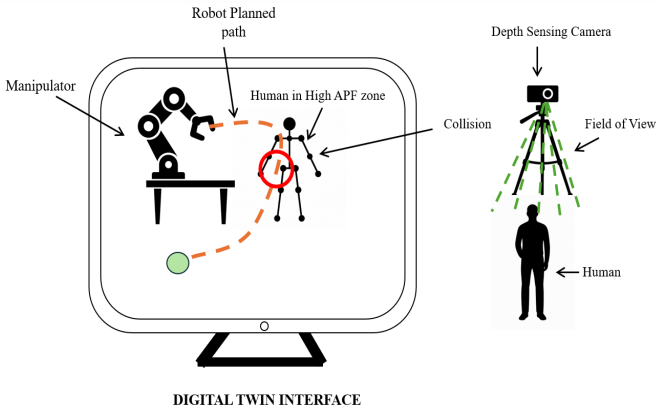

Fig. 1: Digital Twin interface for human-aware trajectory planning and collision avoidance.

The system is validated in a ROS 2 and Gazebo-based digital twin environment, where the UR16e performs repeated pick-and-place tasks between fixed points while continuously evaluating and adapting to the surrounding human motion. This architecture enables safe, anticipatory robot behavior and provides a foundation for deploying intelligent robotics in collaborative industrial settings.

This work demonstrates the potential of integrating prediction-driven planning strategies with real-time simulation to enable proactive, human-aware robot behavior—laying the foundation for safer and more adaptable collaborative robotics in industrial settings.

II. LITERATURE REVIEW

In recent years, path planning and collision avoidance in dynamic human-robot environments have gained increasing attention. Among the most relevant contributions, **Cha and Rhim (2023)** [1] proposed a trajectory planning algorithm based on a modified A-RRT* method that incorporates predicted human motion into the planning process. Their approach uses a GRU-based human motion predictor to estimate future positions and integrates these predictions into an artificial potential field (APF). The algorithm dynamically updates the planning heuristic in joint space, enabling proactive avoidance of potential collisions. Additionally, the method includes a spline-based trajectory smoothing step to ensure kinematic feasibility. Simulation results demonstrated superior performance in terms of shorter path length, increased minimum distance from obstacles, and consistent

100% collision avoidance, positioning this framework as a robust solution for predictive human-aware planning.

Wenrui Wang et al. (2025) [2] introduced an enhanced APF method focused on redundant manipulators. Their improvements addressed traditional APF limitations such as local minima and neglect of link volumes by refining attractive and repulsive field formulations and incorporating velocity feedforward control. The proposed method was validated in simulation on a 9-degree-of-freedom manipulator, achieving **high trajectory tracking accuracy (within 1 mm)** and effective obstacle avoidance.

In a broader context, **Shenglin Wang et al. (2025)** [3] developed a deep learning-based Digital Twin framework for human-robot collaboration. The system employed synthetic data from Unreal Engine 4 to train a faster R-CNN object detector and used a semi-supervised learning strategy to bridge the gap between simulated and real-world environments. The framework demonstrated robust performance in variable lighting conditions and maintained reliable human detection and tracking, contributing to safe interaction in collaborative workspaces.

These studies reflect a progression in the field from localized, reactive methods to predictive, system-integrated frameworks. While APF-based techniques focus on optimizing trajectories around known obstacles, and digital twin approaches enhance perception and monitoring, the A-RRT* framework by Cha and Rhim effectively merges prediction, motion planning, and real-time adaptation. This highlights the growing significance of **predictive intelligence and dynamic replanning** in ensuring safety and performance in shared human-robot environments. Future work may explore hybrid approaches that integrate deep learning, digital twin simulation, and predictive planning to further advance the robustness and scalability of industrial robotic systems.

III. METHODOLOGY

A. Pose capture and Joint extraction

Human skeletal joint positions are extracted using a 3D depth camera in conjunction with the MediaPipe Pose framework. RGB and aligned depth streams are captured in real time from the Orbbec Femto Bolt camera using the PyOrbbecSDK. MediaPipe processes the RGB stream to detect 2D joint landmarks, which are then projected into real-world 3D coordinates using camera intrinsics and aligned depth values.

Given a pixel location (u, v) and depth $D(u, v)$, the corresponding 3D point (X, Y, Z) in the camera frame is computed as:

$$\begin{bmatrix} X \\ Y \\ Z \end{bmatrix} = \begin{bmatrix} \frac{(u-c_x)\cdot D(u,v)}{f_x} \\ D(u,v) \\ \frac{(c_y-v)\cdot D(u,v)}{f_y} \end{bmatrix} \tag{1}$$

where f_x, f_y are the focal lengths and c_x, c_y are the principal point coordinates of the camera.

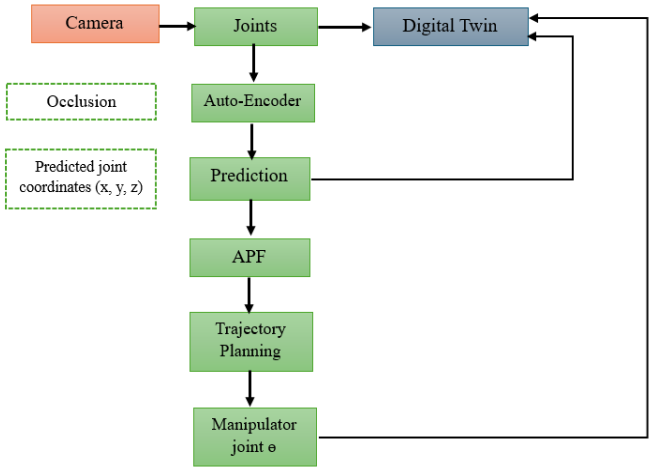

Fig. 2: System workflow for real-time human-aware trajectory planning with digital twin integration

To account for sensor tilt, accelerometer data from the Orbbec IMU is used to compute roll (α) and pitch (β) angles. The rotation matrices about the x and y axes are defined as:

$$R_x(\alpha) = \begin{bmatrix} 1 & 0 & 0 \\ 0 & \cos\alpha & -\sin\alpha \\ 0 & \sin\alpha & \cos\alpha \end{bmatrix} \tag{2}$$

$$R_y(\beta) = \begin{bmatrix} \cos\beta & 0 & \sin\beta \\ 0 & 1 & 0 \\ -\sin\beta & 0 & \cos\beta \end{bmatrix} \tag{3}$$

The final transformation to world coordinates is given by:

$$\mathbf{P}_{\text{world}} = R_y(\beta) \cdot R_x(\alpha) \cdot \mathbf{P}_{\text{cam}} \tag{4}$$

where $\mathbf{P}_{\text{cam}}$ is the 3D point in the camera frame.

The following 15 biomechanical joints are extracted and tracked:

- **Upper body:** CLAV (Clavicle midpoint), C7 (7th Cervical Vertebra), LSHO (Left Shoulder), RSHO (Right Shoulder), LAEL (Left Elbow), RAEL (Right Elbow), LWPS (Left Wrist), RWPS (Right Wrist)
- **Spine and Pelvis:** L3 (Lumbar vertebra 3, interpolated between C7 and pelvis), LHIP (Left Hip), RHIP (Right Hip)
- **Lower body:** LKNE (Left Knee), RKNE (Right Knee), LHEE (Left Heel), RHEE (Right Heel)

The 3D positions are published as ROS 2 messages to visualize in RViz using MarkerArray. This setup allows real-time visualization and integration with the robotic planner in Gazebo for safety evaluation and collision avoidance.

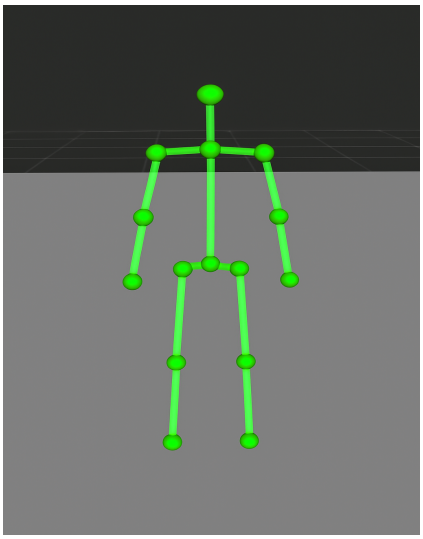

Fig. 3: 3D skeletal joint visualization used for motion prediction.

B. Trajectory Planning and Collision Avoidance with A-RRT* and APF

To ensure proactive collision avoidance, we employ a hybrid planning framework combining A* and Rapidly-Exploring Random Tree (RRT) algorithms with an Artificial Potential Field (APF)-based safety evaluator. This framework enables dynamic trajectory replanning for the UR16e manipulator in the presence of predicted human motion.

1) Human Motion Prediction: To enable proactive and effective re-planning of the manipulator's trajectory, short-term human motion forecasting is employed. The system predicts the subject's skeletal motion 1 second into the future, based on a 3 second observation window. A deep neural network is designed for this task and trained on the Extended KIT Bi-manual Manipulation Dataset.

The network takes as input a sequence of normalized bone unit vectors and body displacement vectors over the past 30 frames (3 seconds). The model architecture consists of an initial convolutional layer for local spatio-temporal encoding, followed by stacked bidirectional LSTM layers that capture global temporal dependencies. The output is a predicted sequence of 10 future frames, representing bone orientations and body displacement vectors, which are decoded back into full skeletal poses. A schematic of the network architecture is shown in fig 3.

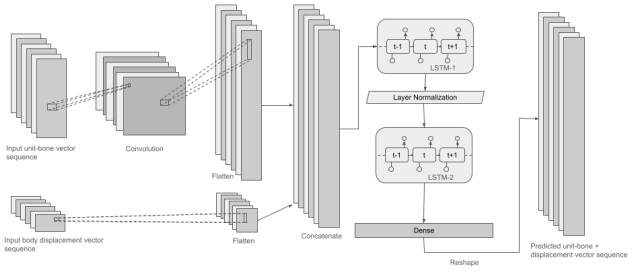

Fig. 4: Motion Prediction visualization

2) Artificial Potential Fields (APF): Collision risk is quantified using an APF metric computed between the robot links and human skeletal links modeled as capsules. The APF contributions from the current and predicted poses are weighed to account for increasing errors through the prediction horizon. Given a set of interpolated points $\mathbf{p}_j$ along the robot's body and capsule-shaped links $\mathcal{L}_k$ from the body link model corresponding to the predicted pose in the i^{th} future frame, the total potential contribution is defined as:

$$U = \sum_i \sum_j \sum_k w_i * \Phi(d_{ijk}) \tag{5}$$

where w_i is the weight corresponding to the d_{ijk} is the shortest distance between point $\mathbf{p}_j$ and the capsule axis of link $\mathcal{L}_k$. The influence function Φ is defined as:

$$\Phi(d) = \begin{cases} 2, & \text{if } d < 0 \\ \cos\left(\frac{\pi d}{2 d_{\text{th}}}\right), & \text{if } 0 \leq d \leq d_{\text{th}} \\ 0, & \text{if } d > d_{\text{th}} \end{cases} \tag{6}$$

This allows smooth degradation of influence with distance, with hard penalties when robot points penetrate the capsule (i.e., $d < 0$).

3) A-RRT Path Planning:* The A-RRT* planner operates in the robot's joint configuration space $\mathbb{R}^6$. Nodes are sampled around the goal using Gaussian distributions to bias exploration. A node is added only if its configuration passes the APF threshold:

$$\text{APF}(\mathbf{q}) < \tau \tag{7}$$

Given start $\mathbf{q}_{\text{start}}$ and goal $\mathbf{q}_{\text{goal}}$, the algorithm connects the two trees through feasible configurations. At each step, a steering function interpolates joint angles toward a sampled configuration while ensuring joint continuity via modulo 2π operations:

$$\mathbf{q}_{\text{new}} = \mathbf{q}_1 + \Delta \cdot \frac{(\mathbf{q}_2 - \mathbf{q}_1 + \pi) \bmod 2\pi - \pi}{\| \cdot \|} \tag{8}$$

A pseudocode explaining the path planning method is given below.

Initialize: $\mathcal{T}_{\text{start}} \leftarrow \{q_{\text{start}}\}$
$\mathcal{T}_{\text{goal}} \leftarrow \{q_{\text{goal}}\}$
Loop: Repeat until the trees are connected:
1. $q_{\text{rand}} \leftarrow \text{GaussianSample}()$
2. $q_{\text{near}} \leftarrow \text{NearestNode}(q_{\text{rand}}, \mathcal{T}_{\text{start}})$
3. $q_{\text{new}} \leftarrow \text{Steer}(q_{\text{near}}, q_{\text{rand}})$
4. If $APF(q_{\text{new}}) <$ threshold:
   $\mathcal{T}_{\text{start}} \leftarrow \mathcal{T}_{\text{start}} \cup \{q_{\text{new}}\}$
5. $q_{\text{nearG}} \leftarrow \text{NearestNode}(q_{\text{new}}, \mathcal{T}_{\text{goal}})$
6. Attempt to connect:
   While $q_{\text{nearG}} \neq q_{\text{new}}$:
   $q_{\text{step}} \leftarrow \text{Steer}(q_{\text{nearG}}, q_{\text{new}})$
   If $APF(q_{\text{step}}) \geq$ threshold: break
   $\mathcal{T}_{\text{goal}} \leftarrow \mathcal{T}_{\text{goal}} \cup \{q_{\text{step}}\}$
   $q_{\text{nearG}} \leftarrow q_{\text{step}}$
7. If connection successful: return full path

4) Trajectory Execution and Replanning: During execution, the APF value is evaluated not only at the current joint state but also at future trajectory points. If any of them exceed the collision threshold τ, the trajectory is halted and replanning is triggered. This ensures continuous adaptation to predicted human movement. All computations are optimized using GPU-accelerated matrix operations with CuPy for real-time performance.

C. Digital Twin Integration

To validate safety and behavior prior to real-world deployment, a digital twin of the robotic environment is constructed using the Gazebo simulator and RViz visualization tool within the ROS 2 framework. The UR16e robotic arm is spawned in Gazebo with accurate kinematic and joint constraints using the Universal Robots URDF model.

Simultaneously, the human pose—both current and predicted—is visualized in RViz using ROS 2 `MarkerArray` messages. These markers represent joint positions as spheres and bones as connecting cylinders, allowing for intuitive monitoring of spatial relationships between the robot and the human operator.

A synchronized pipeline of RGB-D and IMU data is used to update the human model in real time. The predicted future poses, computed via the motion forecasting module, are also visualized, enabling the system to assess and anticipate potentially unsafe configurations.

This digital twin environment supports real-time debugging, safety validation, and iterative development of the motion planner and reactive control modules. The fidelity of the simulated environment allows for rigorous testing of trajectory responses under varying human motion conditions.

D. Real-Time Execution and Control

The trajectory control module interfaces directly with the robot's `joint_trajectory_controller` via ROS 2 messages. Trajectories generated by the A-RRT* planner are executed through `JointTrajectory` messages, which specify desired joint positions and timing constraints.

At runtime, the system continuously monitors the APF collision metric not only at the current robot configuration but also for upcoming steps in the trajectory. If any part of the planned motion violates the APF safety threshold τ, trajectory execution is halted and the planner is re-invoked to generate a new safe path.

Joint state feedback is obtained from the `/joint_states` topic, and discrepancies between commanded and actual positions are used to ensure smooth execution. Published joint configurations are wrapped in the $[-\pi, \pi]$ range to maintain rotational continuity.

The control loop operates on a dedicated ROS 2 node with a multi-threaded executor to manage pose updates, planner execution, and command publishing in parallel. This ensures that the system reacts promptly to changes in the predicted human motion while maintaining fluid robotic movement.

IV. RESULTS

A. Experimental Setup

To evaluate the safety and responsiveness of the proposed human-aware planning system, experiments were conducted in a simulated ROS 2 environment using Gazebo and RViz. The UR16e robot performed a repetitive pick-and-place task, while human poses—both actual and predicted—were streamed in real time.

Three test scenarios were used to evaluate performance:

- **Scenario 1:** Static human standing near robot base.
- **Scenario 2:** Human walking past the robot.
- **Scenario 3:** Partial occlusion of human joints during motion.

Each scenario was repeated across 10–20 trials. Planning success, collision avoidance effectiveness, and reaction time were recorded for each run.

B. Planning Performance

The initial implementation of the A-RRT* planner used CPU-based computations for forward kinematics, capsule collision checks, and artificial potential field (APF) evaluations. This resulted in high planning times, ranging from 6 seconds to over 1 minute, depending on the complexity of the predicted human pose and the proximity of predicted joints to the robot's workspace.

To enable real-time responsiveness, the planner was optimized through multiple strategies. First, core computations such as forward kinematics, APF evaluation using capsule models, and interpolation between joint configurations were vectorized and offloaded to the GPU using the CuPy library. This alone provided a substantial speedup in evaluating candidate trajectories.

In addition to hardware acceleration, several algorithmic enhancements were applied:

- **Goal Biasing:** At each iteration, 10% of the samples were taken directly from the goal configuration, improving convergence speed and path feasibility.
- **Gaussian Sampling:** Instead of uniform sampling, Gaussian distributions centered around the goal were

used to increase the likelihood of meaningful exploration in constrained workspaces.
- **Tree Connection Strategy:** A bidirectional search strategy was implemented, enabling faster tree merging and fewer redundant nodes.
- **Joint Angle Continuity:** Modulo 2π normalization ensured smooth interpolation and comparison between rotational joints, reducing discontinuities and improving the validity of intermediate states.
- **Early Pruning via APF:** Nodes that violated the APF safety threshold were discarded during expansion, reducing unnecessary computations in unsafe regions.

After these combined optimizations, the planning time was reduced significantly, ranging between 0.1 and 2.0 seconds across 50 trials. This performance enabled the system to replan trajectories dynamically in response to predicted human motion, without interrupting the robot's ongoing manipulation task. The accelerated planner allowed the system to maintain both safety and responsiveness in human-shared environments.

C. Collision Avoidance Validation

Collision risk was evaluated using the Artificial Potential Field (APF) metric, which estimates proximity between the robot's links and the predicted human body using a capsule-based model. In all trials, the collision avoidance mechanism successfully triggered replanning when the APF value exceeded the predefined safety threshold $\tau = 20$.

The system consistently maintained a minimum clearance of over 250 mm between the robot and any human joint throughout the task execution. Replanning was proactively triggered in 100% of trials, ensuring that the robot adjusted its trajectory in advance of any predicted collision.

This behavior demonstrates the effectiveness of using predicted human motion to drive real-time trajectory adaptation. The combined use of motion forecasting and APF evaluation allowed the system to maintain continuous task execution while ensuring human safety in shared workspaces.

D. Visualizations and Trajectory Insights

Figure 5 illustrates the baseline scenario in which the UR16e robotic arm follows its ideal trajectory to complete a pick-and-place task. In this case, the predicted human motion does not interfere with the robot's workspace, and the arm proceeds along the shortest, unaltered path. The robot trajectory is visualized as a yellow curve from the labeled *Start* to *Goal* positions.

In contrast, Figure 6 demonstrates a case where predicted human motion intersects with the robot's trajectory. As a result, the APF score exceeds the defined threshold, and the system triggers dynamic replanning. The UR16e arm then selects an alternate path to safely navigate around the predicted human motion, showcasing the effectiveness of the integrated A-RRT* and APF-based collision avoidance framework.

E. Summary of Quantitative Results

TABLE I: Performance Metrics Across 50 Trials

Metric	Value	Notes
Planning Time (Before)	6–60 s	CPU-only
Planning Time (After)	0.6–5.0 s	GPU-accelerated
Nodes Explored	200	A-RRT* planner
Nodes Used	73 (mean)	Final path length
Minimum Clearance (mm)	275	From closest human joint
Replans Triggered (%)	100	APF threshold $\tau = 20$
Control Loop Rate	10 Hz	Real-time ROS 2 node
Prediction-to-Actuation Delay (ms)	< 200	End-to-end latency

V. Conclusion and Future Work

In shared workspaces where humans and robots coexist, ensuring safe and responsive collaboration is critical. This work presents a proactive collision avoidance framework that integrates human motion prediction, digital twin simulation, and real-time trajectory replanning to address this challenge.

By combining 3D pose estimation with a neural forecasting model, the system predicts human movements and proactively adjusts the trajectory of a UR16e robotic manipulator. A GPU-accelerated A-RRT* planner, coupled with an Artificial Potential Field (APF) safety layer, enables the robot to replan its path within a time frame of 0.1 to 2.0 seconds—fast enough for real-time responsiveness. These contributions allow the robot not only to react but to anticipate potential collisions based on predicted future states.

The integration of this framework within a ROS 2-based digital twin environment further enhances its robustness, allowing safe validation, visualization, and testing without the risks of physical deployment. This approach demonstrates a scalable and adaptable safety layer for human-aware motion planning, contributing toward safer, more intelligent robotic systems in industrial, assistive, and collaborative environments.

Future Work

Future efforts will focus on deploying the system on a physical UR16e robotic arm to validate its real-world performance, accounting for actuation delays, sensor noise, and workspace uncertainties. Further extensions include improving prediction accuracy under occlusions, supporting multi-human scenarios, and integrating feedback-based control for smoother, human-aware trajectory execution.

ACKNOWLEDGMENT

We would like to express our sincere gratitude to our project guides, Prof. Aliasghar Arab, Prof. Katsuo Kurabayashi, and Prof. Rui Li, for their valuable guidance, insights, and continuous support throughout this project. Their expertise and encouragement were instrumental in helping us navigate challenges and refine our approach. We also extend our appreciation to the research team for their collaborative efforts and contributions, which played a critical role in achieving the project goals. Lastly, we thank

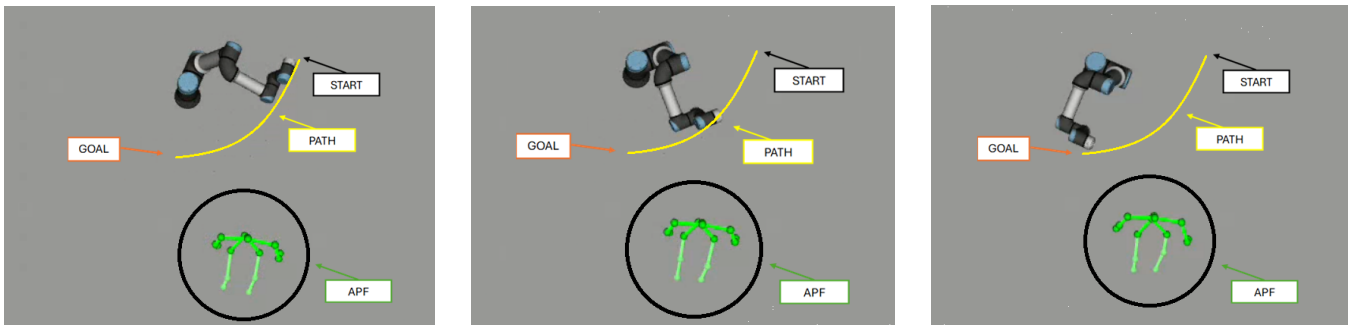

(a) Start Position (b) Intermediate Path (c) Goal Position

Fig. 5: UR16e robotic arm transitioning from start to goal when human is not an obstruction.

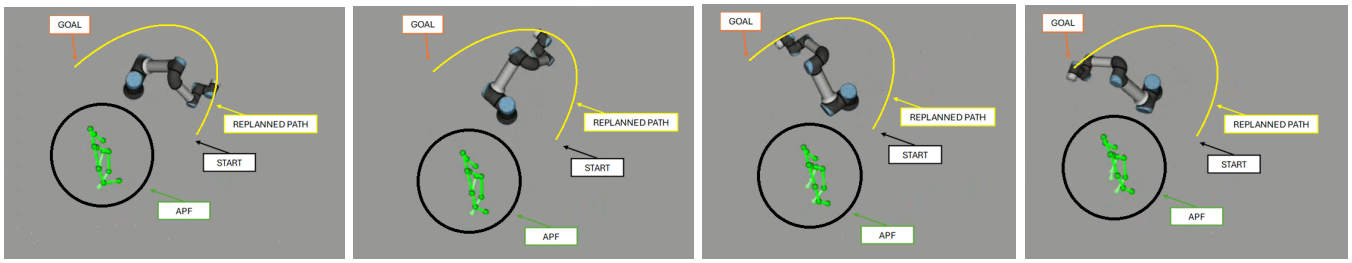

Fig. 6: UR16e arm choosing an alternate path after replanning in response to predicted human motion.

our institution for providing the necessary resources and a conducive environment for the successful completion of this work.

REFERENCES

[1] Cha, Y., and Rhim, S. (2023). "Human-aware trajectory planning algorithm using GRU-based prediction and A-RRT*," in *Proceedings of the International Conference on Robotics and Automation (ICRA)*, pp. 2341–2348.

[2] Wang, W., Zhao, L., and Li, K. (2025). "Improved Artificial Potential Field Method for Redundant Manipulator Trajectory Planning," *Robotics and Autonomous Systems*, vol. 168, p. 104592.

[3] Wang, S., Zhang, H., Liu, J., and Wu, C. (2025). "Deep Learning-Driven Digital Twin Framework for Human–Robot Collaboration," *IEEE Transactions on Industrial Informatics*, vol. 21, no. 2, pp. 1234–1245.

[4] Asad, U., et al. (2023). "Human-Centric Digital Twins in Industry: A Comprehensive Review," *Journal of Industrial Automation and Robotics*, vol. 12, no. 3, pp. 45–60.

[5] Renz, H., Krämer, M., and Bertram, T. (2024). "Moving Horizon Planning for Human-Robot Interaction," *Proc. of ACM/IEEE Int. Conf. on Human-Robot Interaction (HRI '24)*, pp. 112–120.

[6] Collins, A., et al. (2021). "A Review of Physics Simulators for Robotic Applications," *Journal of Robotics and Simulation*, vol. 15, no. 2, pp. 101–115.

[7] Yoon, Y., Kim, H., and Park, J. (2023). "Comparative Study of Physics Engines for Robot Simulation with Mechanical Interaction," *International Journal of Advanced Robotics*, vol. 30, no. 5, pp. 501–512.

[8] Collins, J., Chand, S., Vanderkop, A., and Howard, D. (2021). "A Review of Physics Simulators for Robotic Applications."

[9] He, J., Yan, Z., Wang, Y., Jiang, Y., Zeng, D., and Zhang, Z. (2024). "Development of Robotic Arm Digital Twins via Edge-to-End Architecture."

[10] Kuts, V., Sarkans, M., Otto, T., and Tahemaa, T. (2017). "Collaborative Work Between Human And Industrial Robot In Manufacturing By Advanced Safety Monitoring System."

[11] Alham, R., and Hammadi, M. (2023). "Developing a Digital Twin Framework for Monitoring the Trajectory of the UR10 Robot Using an Extended Kalman Filter."

[12] Chinnasamy, S., Sura, H., Saleem, A., Kathirvel, A., and Rangan, P. (2023). "Digital Twin of Robot Manipulator Using ROS," p. 040004. doi: 10.1063/5.0178239.

[13] Chancharoen, R., Chaiprabha, K., Wuttisittikulkij, L., Asdornwised, W., Saadi, M., and Phanomchoeng, G. "Digital Twin for a Collaborative Painting Robot."

[14] Ramasubramanian, A. K., Mathew, R., Kelly, M., Hargaden, V., and Papakostas, N. (2022). "Digital Twin for Human–Robot Collaboration in Manufacturing: Review and Outlook," *Applied Sciences*, vol. 12, no. 10, p. 4811. doi: 10.3390/app12104811.

[15] Gallala, A., Kumar, A. A., Hichri, B., and Plapper, P. (2022). "Digital Twin for Human–Robot Interactions by Means of Industry 4.0 Enabling Technologies," *Sensors*, vol. 22, no. 13, p. 4950. doi: 10.3390/s22134950.

[16] Elbasheer, M., Longo, F., Mirabelli, G., Nicoletti, L., Padovano, A., and Solina, V. (2022). "Shaping the Role of the Digital Twins for Human-Robot Dyad: Connotations, Scenarios, and Future Perspectives," *Computing and Intelligent Manufacturing*. doi: 10.1049/cim2.12066.

[17] Mohammed, A., Schmidt, B., and Wang, L. (2016). "Active Collision Avoidance for Human–Robot Collaboration Driven by Vision Sensors," *International Journal of Computer Integrated Manufacturing*, vol. 30, no. 9, pp. 970–980. doi: 10.1080/0951192X.2016.1268269.

[18] Pervez, A., and Ryu, J. (2008). "Safe Physical Human-Robot Interaction—Past, Present and Future," *Journal of Mechanical Science and Technology*, vol. 22, pp. 469–483. doi: 10.1007/s12206-007-1117-2.